

Auger Electron-Ion Coincidence Studies to Determine the Pathways in Soft X-ray Induced Fragmentation of Isolated Molecules*

W. Eberhardt,^A E. W. Plummer,^B In Whan Lyo,^B R. Reininger,^B
R. Carr,^C W. K. Ford^D and D. Sondericker^E

^A Exxon Research and Engineering Company, Clinton Township,
Route 22 E, Annandale, NJ 08801, U.S.A.

^B Department of Physics, University of Pennsylvania,
Philadelphia, PA 19104, U.S.A.

^C SSRL, P.O. Box 4349 Bin 69, Stanford, CA 94305, U.S.A.

^D Physics Department, Montana State University, Bozeman, MT 59717, U.S.A.

^E National Synchrotron Light Source, Brookhaven National Laboratory,
Upton, NY 11973, U.S.A.

Abstract

We report a coincidence experiment between energy selected Auger electrons and the ions produced in the events following the absorption of a soft X-ray photon by a CO molecule. This study allows us to correlate specific double hole final state configurations of the Auger decay of a core hole in this molecule with the production of fragment ions, thus giving new experimental insight into the potential energy curves of the doubly charged molecular ion and the involvement of individual valence electrons into the molecular bond in general.

1. Introduction

Absorption of a soft X-ray photon by an isolated molecule leads to a chain of events, the end result of which is the production of ionic fragments of the parent molecule (Eberhardt *et al.* 1983*a*, 1983*b*, 1985). In general the absorption of the photon leads to the creation of a neutral or ionic core hole excited state, which is still a stable configuration. The subsequent decay of the core hole state occurs preferentially via a radiationless Auger type transition, since the fluorescence yields for the light elements we are studying are very low. This radiationless decay depletes the bonding structure of the molecule of electrons such that fragmentation into ions occurs. In our previous studies (Eberhardt *et al.* 1983*a*) we showed that the fragmentation occurs site specific, i.e. the molecule falls apart around the atomic centre where the initial core hole was created. The branching ratio of the fragments also depends critically on the photon energy near the onset of the core electron absorption and specifically on the nature of the core hole excited state (Eberhardt *et al.* 1983*b*, 1985). We established a correlation between the various electronic final state configurations observed in the decay of the core hole excited state and certain fragmentation channels (Eberhardt *et al.* 1983*b*, 1985). The missing link, however, in these studies was a direct coincidence measurement between each of the various Auger final states and the ions associated with this specific hole configuration.

* Paper presented at the Specialist Workshop on Excited and Ionised States of Atoms and Molecules, Strathgordon, Tasmania, 3-7 February 1986.

We present here a step-by-step analysis of the events leading to the fragmentation of CO. Using the direct quasi-monochromatic soft X-ray beam of the SSRL beam line V undulators we had sufficient intensity to perform the coincidence studies mentioned above. At 3 GeV electron energy the fundamental of one of the undulators could be scanned between 1200 and 800 eV, thus we were able to perform the coincidence studies for the events that follow the ionisation of a core electron. A second magnet configuration allowed the fundamental to be tuned between 300 and 600 eV, giving access to the core threshold region at the C and O K-edge.

2. Experimental Setup

The experimental setup has been described previously (Eberhardt *et al.* 1984). The ions are detected with a time-of-flight (TOF) mass spectrometer and the electron detector is a CMA electron spectrometer. Both are oriented with their axes on opposite sides and perpendicular to the plane of the X-ray beam and the molecular gas beam. Whenever an electron is detected in the CMA it starts a TDC (time-to-digital converter) which is stopped by pulses coming from the ion mass spectrometer. The time difference between the two pulses is related to the mass of the ion and its initial kinetic energy.

With this setup we can study the chain of events leading from the absorption of the soft X-ray photon to the production of ions. Measuring either the total electron yield or the total ion yield as a function of photon energy, we get a curve that closely resembles the absorption spectrum of the molecules. At any given photon energy we can measure the distribution curve of the electrons produced in the core hole decay with the CMA. The fragment mass spectra are accumulated by triggering on the unresolved Auger electron signal seen by a channeltron with a retarding grid in place of the electron spectrometer. Using an electron energy analyser instead of the channeltron in the latest experiment configuration, we can tune into the individual lines of the Auger spectrum and measure the ions in coincidence with this specific Auger decay, thus correlating individual two hole final state configurations with the observation of certain ionic fragments.

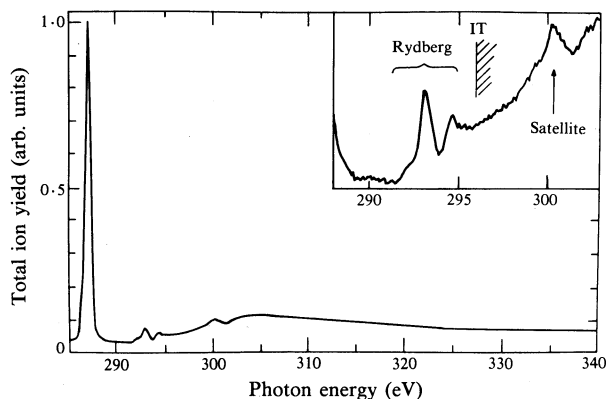


Fig. 1. Total ion yield of CO near the onset of the C_{1s} excitation. The total ion yield closely resembles the absorption and shows structures due to C_{1s} transitions into various types of final states.

3. Core Electron Excitation and Fragmentation

We begin by presenting some results which indicate that the fragmentation events clearly depend on the details of the initial electronic excitation. The various types of core electron excitations are illustrated in Fig. 1, where we show the total ion yield of CO measured as a function of the photon energy near the onset of the C_{1s} transitions. This spectrum is very similar to, but not as well resolved as, electron energy loss spectra in the literature (Hitchcock and Brion 1980; Shaw *et al.* 1984). Nevertheless the main features due to the various types of electronic transitions of the C_{1s} core electron are well resolved. The strongest feature at 287.3 eV, well below the ionisation threshold (IT) of the C_{1s} electron in CO at 296.1 eV, corresponds with a transition of the C_{1s} electron into the lowest unoccupied molecular orbital, the 2π orbital. At slightly higher energies than this π^* transition we see transitions into Rydberg type orbitals converging to the ionisation threshold. The peak at 300.5 eV is commonly interpreted as due to a two electron transition resulting in a $1s^{-1}1\pi^{-1}2\pi^2$ final state configuration.

The differences in the ion mass spectra for these various core hole excited states are illustrated in Fig. 2. We also include a mass spectrum taken with 140 eV photons, where only direct valence electron excitations cause the fragmentation. At this photon energy the dominant species is CO^+ . At the higher photon energies, near the core electron absorption edges, the valence excitation cross sections are very small. For example, at 305 eV the sum of all the valence excitations contributes less than 10% to the total absorption cross section (Kay *et al.* 1977). The curves in Fig. 2 clearly demonstrate the effect of the initial excitation on the branching ratio of the ionic fragments. After core excitation or ionisation the weight of the mass spectra shifts to the fragments rather than the undissociated CO^+ ion and even for the different types of core excitation we observe distinct differences in the fragment spectra.

The appearance of doubly charged species, C^{2+} or O^{2+} , below the core ionisation threshold is at first glance unexpected. The decay of the core hole excitation will, in general, leave the molecule in a singly charged state. In order to account for doubly charged fragments, a secondary decay process has to occur. The appearance of these fragments at a photon energy of 140 eV, however, is even more surprising. These fragments can only result from either a shake-off event in the initial photoionisation process or a shake-up configuration of the 3σ inner valence hole state. For energetic reasons there is no possibility for a single valence hole configuration to decay via an Auger decay. The double ionisation potential of CO is 41 eV, several eV higher than the single particle binding energy of a 3σ inner valence hole, which is 38 eV.

Before we attempt to correlate the production of certain fragments with valence electronic configurations populated in the Auger type decay of the core hole, we will briefly discuss the fine structure in the mass spectra. A high resolution scan of the mass spectra across the range where C^+ and O^+ are recorded is shown in Fig. 3. The central CO^{2+} peak contains only ions with thermal energies and its width is equivalent to our total time resolution of 15 ns. Most of the fragment ions, on the other hand, are produced in a 'Coulomb explosion' and therefore have a large kinetic energy and momentum. These mass peaks show considerable broadening, because the ions starting in the direction of the detector along its axis arrive first, next the ions with momentum components perpendicular to the detector axis are detected and finally the ions are recorded which initially moved away from the detector and then were turned

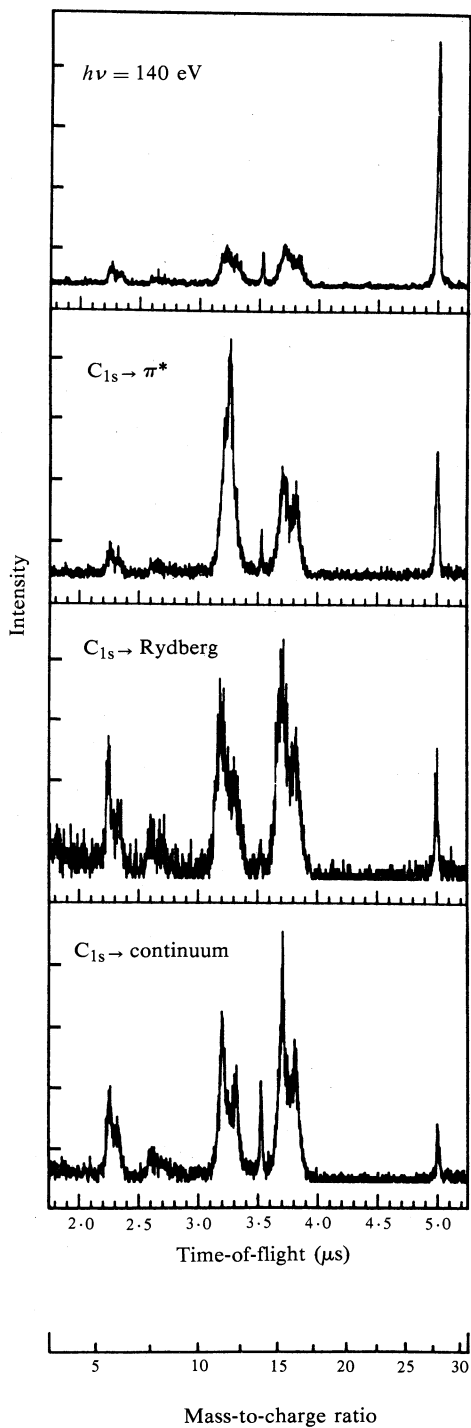


Fig. 2. The CO fragment ion mass spectra measured with a TOF mass spectrometer. The spectra are taken at different excitation energies to reflect the effect of the primary excitation on the branching ratio of the ionic fragments.

around in the extraction field. Apertures within the TOF mass spectrometer will, for an isotropic momentum distribution, first affect the ions moving perpendicular to its axis; this causes the characteristic double-peak structure seen in the spectra. In an ion-ion coincidence experiment we have also verified that part of the C^+ ions are correlated with the O^+ ions and therefore are generated in the same event. In this ion-ion coincidence experiment we observed coincidences corresponding to the time difference between the first C^+ ions and the last O^+ ions and vice versa.

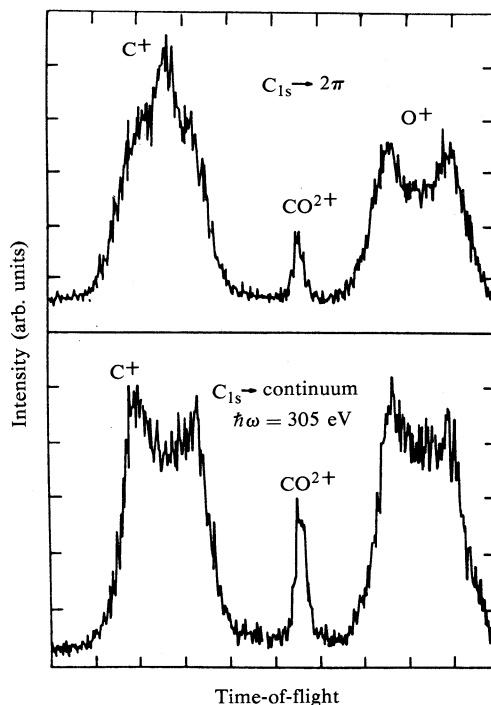


Fig. 3. High resolution mass spectrometer scan from $m/e = 12-16$. The sharp peak in the centre is due to CO^{2+} having only thermal energy. The other peaks show substructure and substantial broadening due to the kinetic energy distribution of the fragments.

Comparing the actually measured TOF mass spectra with model calculations for our TOF detector, we can estimate the kinetic energies of the fragments. In general the ions have several eV of kinetic energy.

4. Core Hole Decay as an Intermediate Step

So far we have dealt with the characterisation of the initial photon absorption event and the final product distribution. The intermediate step, however, which determines the pathway for the fragmentation, is the electronic decay of the neutral or ionic core hole excited state. The spectrum of the electrons created in the decay of the $C_{1s} \rightarrow 2\pi$ excitation and the spectrum following C_{1s} ionisation are compared

in Fig. 4. A certain similarity between these two spectra is clearly recognisable. The differences are due to differences in the total ionisation state and changes in the multiplet splitting in the individual final states. The deexcitation starts with the molecule in the neutral state, whereas the Auger transition starts in an ionised system and ends with a doubly ionised state.

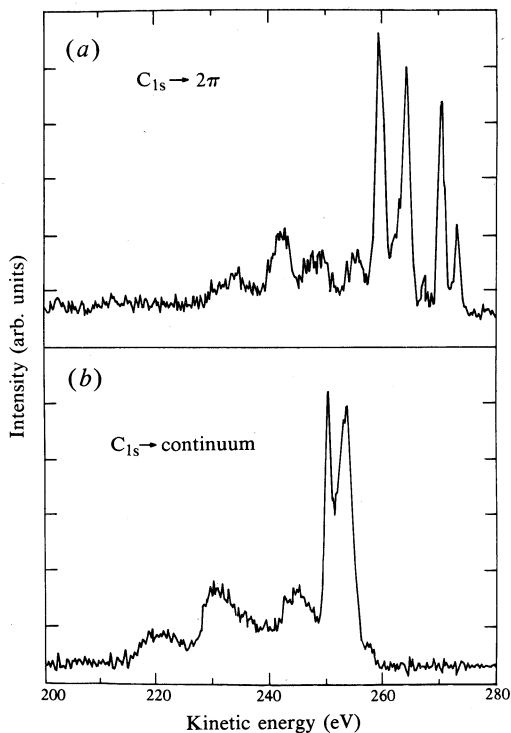


Fig. 4. Electron energy distribution curves of the electrons created in the decay of the primary C_{1s} core hole excited state in CO. In (a) the decay of the $C_{1s} \rightarrow 2\pi$ excitation is shown, while (b) shows the 'standard' Auger spectrum following C_{1s} ionisation.

Most of the Auger lines have been assigned empirically (Siegbahn *et al.* 1969; Moddeman *et al.* 1971) or based on detailed calculations of the binding energies of the final state hole configurations (Ågren and Siegbahn 1980; Kelber *et al.* 1981; Liegener 1984; Laramore 1984; Correia *et al.* 1985). The assignment for the various Auger lines is given in Table 1. The spectrum produced in the decay of the $C_{1s} \rightarrow 2\pi$ excitation was also partially observed in electron excited Auger spectra and the assignment was discussed by Moddeman *et al.* (1971) and Correia *et al.* (1985). The assignment for the deexcitation (DES) spectra derived in our previous work (Eberhardt *et al.* 1986; p. 853, present issue) is also shown in Table 1.

The Auger and DES spectra are an indirect proof that the molecule is still intact after the initial photoabsorption event that leads to the core electron excited state and that the key step is the core hole decay. This is not surprising, since the core hole lifetime is about 10^{-14} s which is much shorter than the nuclear motion and

dissociation. Our aim is now to correlate the individual final state configurations of the CO molecule after the Auger transition or deexcitation with the various fragmentation channels. This will be done by measuring the fragment mass spectra in coincidence with a selected final state configuration. We only trigger the timing of our TOF mass spectrometer when we observe an Auger electron of a specifically selected kinetic energy. However, before we discuss these coincidence spectra, we will present some simple energy conservation arguments that allow us to make an educated guess about what we expect to observe in the coincidence experiment.

Table 1. Final electronic states of CO

$C_{1s} \rightarrow 2\pi$ (deexcitation)		$C_{1s} \rightarrow \text{continuum}$ (Auger decay)	
E (eV)	Config.	E (eV)	Config.
273.3	$5\sigma^{-1}$	254	$5\sigma^{-2} X^1\Sigma$
270.5	$1\pi^{-1}$	253	$5\sigma^{-1}1\pi^{-1} A^1\Pi$
267.5	$4\sigma^{-1}$	250.5	$4\sigma^{-1}5\sigma^{-1} B^1\Sigma$
264.3	$5\sigma^{-1}1\pi^{-1}2\pi$ or $5\sigma^{-2}2\pi$	245	$4\sigma^{-1}1\pi^{-1}$
259.5	$5\sigma^{-1}1\pi^{-1}2\pi$ or $4\sigma^{-1}5\sigma^{-1}2\pi^A$	230	$3\sigma^{-1}5\sigma^{-1}$
255.5	$4\sigma^{-1}1\pi^{-1}2\pi$	221	$3\sigma^{-1}4\sigma^{-1}$ or $3\sigma^{-1}1\pi^{-1}$
248	$3\sigma^{-1}$	248 ^B	$1\pi^{-2} \Delta \Sigma$
242.5	$3\sigma^{-1}5\sigma^{-1}2\pi^A$	239 ^B	$4\sigma^{-2}$
235	$3\sigma^{-1}1\pi^{-1}2\pi$ or $3\sigma^{-1}4\sigma^{-1}2\pi^A$		

^A These assignments are based on an analogy between the Auger and DES spectra and have no equivalent in the photoemission spectrum.

^B These transitions are very weak in the C Auger spectrum; the transition energy is taken from Moddeman *et al.* (1971).

We can theoretically predict the thresholds for fragments using an adiabatic energy cycle. Starting with the molecule in the ground state we add the energy deposited by the absorption of the soft X-ray photon. This energy corresponds to either the bound state transition energy or the core electron ionisation potential. Any excess energy is immediately carried away by the primary photoelectron ejected in the process. This core hole excited state decays ejecting a second electron, the Auger electron as it is called after core ionisation, removing most of the energy from the system. On the other hand, we also can calculate adiabatically the energy needed to dissociate the molecule into neutral fragments and then ionise part of or all of these neutral fragments individually. These energies are tabulated in the literature (Moore 1958). Closing the energy cycle, we know that a specific fragmentation channel is only open if the Auger electron has carried less energy out of the system than is needed to adiabatically produce these fragments. This is graphically illustrated in Fig. 5 for both the C and O Auger spectra of CO. Only Auger events and consequently the associated two hole final state valence configurations to the left of the thresholds indicated in Fig. 5 can contribute to the individual fragmentation channels. Otherwise the Auger electron has removed too much energy from the system and the channel is closed. We also recognise immediately one shortcoming of the adiabatic scheme to calculate

the thresholds. If both fragments are ionic, there is an additional Coulomb repulsion between the two holes involved, when the two partners are close to each other. This means that the actual thresholds for these channels have to be several eV higher. As the two ions separate, the Coulomb energy is mostly transformed into kinetic energy of the fragments. The term 'Coulomb explosion' arises from these unusually large energies. Measuring these kinetic energies for the fragments therefore allows us also to keep track of the 'hidden' internal energy of the fragments, which could be present in terms of electronic excitations within the individual fragment ions. On the other hand, these electronic excitations are discreet and limited, therefore we do not expect that the fragmentation channels remain open for all energetically possible Auger events as indicated in Fig. 5.

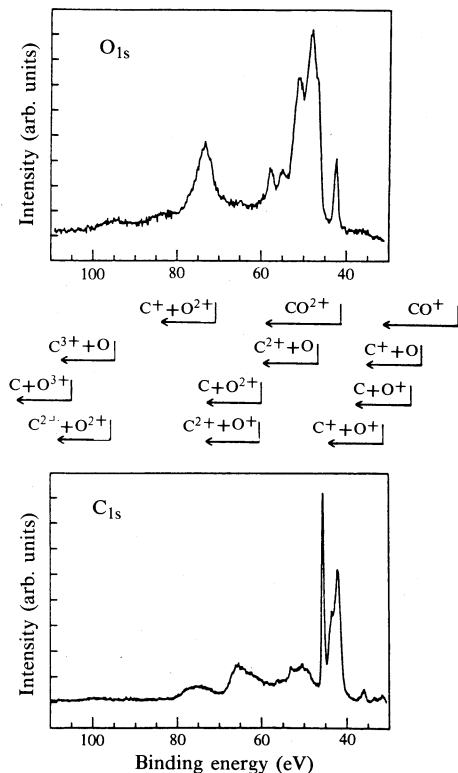


Fig. 5. The CO oxygen and carbon Auger spectra and adiabatic energy thresholds for the production of various ionic fragments. An Auger electron and the corresponding double hole configuration that is found to the right of any one of the thresholds cannot be associated with that particular fragmentation channel because it has carried too much energy out of the system.

Several of the Auger spectra presented in this paper (Figs 5, 7 and 8) are plotted on a binding energy scale. This scale is derived by taking the difference between the kinetic energy of the Auger electrons and the energy of the core hole excited state. This energy is given by the ionisation potential of the core hole in the case of the standard Auger decay or by the transition energy of the core to bound state excitation for the decay of that particular configuration.

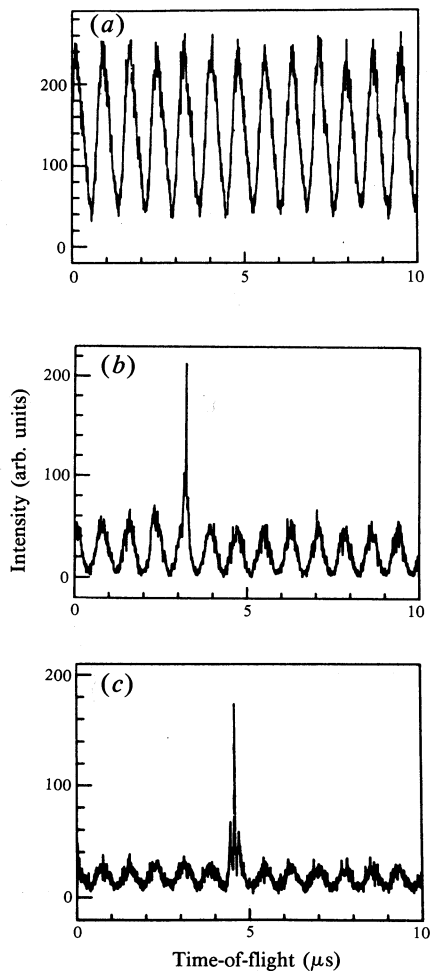


Fig. 6. Auger electron-ion coincidence spectra for N_2 as a function of delay time between the two pulses. In (a) the total intensity is too high and therefore the spectrum is totally dominated by accidental coincidences showing the time structure of the synchrotron source. In (b) the total intensity is reduced and the truly coincident N^+ ions show up. This is verified by lowering the ion acceleration voltage in (c), where the true coincidences appear at larger flight times as expected.

5. Auger Electron-Ion Coincidence Studies

We now test the predictions in Section 4 by actually performing the coincidence experiment. One experimental difficulty in any coincidence experiment is to differentiate between true and accidental coincidences. Using a pulsed source makes this problem even more severe since the accidental coincidences carry the time structure of the source. From theory we know that the accidental coincidences are proportional to the product of the count rates in both channels, i.e. they are proportional to the square of the incoming photon intensity. The true coincidences, however, vary

linearly with the photon flux. Consequently we can increase the ratio of the true to accidental coincidences by lowering the incoming photon flux. Ideally the true to accidental rate is best at zero intensity. In practice, however, noise contributes to a general background and we have to keep a very delicate balance between having too high an intensity and being swamped by accidental coincidences and having insufficient intensity such that the real signal is buried by the general noise. This is accomplished by inserting filters into the X-ray beam or adjusting the gas pressure. Under well adjusted conditions the true coincidences are clearly distinguished from the machine structure background with a ratio of about 20 : 1. This is illustrated by the coincidence spectra shown in Fig. 6. In (a) the spectrum shows a condition where we are completely swamped by accidental coincidences. Lowering the total intensity we record a spectrum as shown in (b), where what we believe to be true coincidences show up as three rather sharp peaks above the machine structure background. This assignment is verified by lowering the ion acceleration voltages which causes the truly coincident events to shift to larger flight times as shown in (c). In subsequent spectra presented in this paper we have removed the time-structure background by subtracting from the measured spectrum a time-shifted part of the spectrum containing only accidental coincidences. This technique seems to work rather well and certainly improves the signal-to-background ratio in our curves such that we are able to discern even weak true coincidence features rather well.

Fig. 7 shows a series of Auger electron-ion coincidence spectra of CO taken in coincidence with the oxygen Auger electrons. The undulator was set to deliver a photon spectrum peaked around 1200 eV for this experiment. Due to the quasi-monochromatic nature of the undulator radiation we only see events corresponding to the initial ionisation of a core electron even though we used the 'white beam' without any additional monochromatisation. The TOF ion mass spectra (c) and (d) are shown at high resolution around the regions where a C^+ or O^+ ion (d) or a C^{2+} or O^{2+} ion (c) is expected to arrive. The background of the accidental coincidences was removed as described above. These are the only clear peaks observed in the coincidence spectra. The mass 28 peak, which corresponds to undissociated, singly ionised CO^+ , and triply or higher charged species are too weak to be observed above the background level in events involving O_{1s} ionisation. As discussed above, the singly charged parent ion is due to direct photoionisation of the valence electrons. At the O edge the ratio between the O_{1s} absorption cross section and the sum of the cross sections of all valence excitations has even shifted more in favour of the core excitation than at the C K-edge.

The TOF spectra were taken in coincidence with Auger electrons as marked by the arrows A-E in the Auger spectrum displayed in Fig. 7b. In order to record the ion TOF spectra we had to apply an electric field across the interaction region, which in turn smears the energy distribution of the Auger electrons. Figs 7a and 7b show, respectively, the Auger spectrum taken in the normal mode, without an electric field across the interaction region, and with the ion extraction field applied. The major features of the Auger spectrum, however, are still visible in (b) and, as the coincidence spectra show, it is even sensitive to the substructure in the major peaks.

The highest kinetic energy Auger electrons, giving rise to the sharp peak on top of the Auger spectrum (Fig. 7), are assigned to correspond predominantly with the $A^1\Pi$ state of CO^{2+} (Correia *et al.* 1985) with a small contribution from the $X^1\Sigma$ molecular ground state of CO^{2+} . In a single particle notation the $A^1\Pi$ state corresponds to

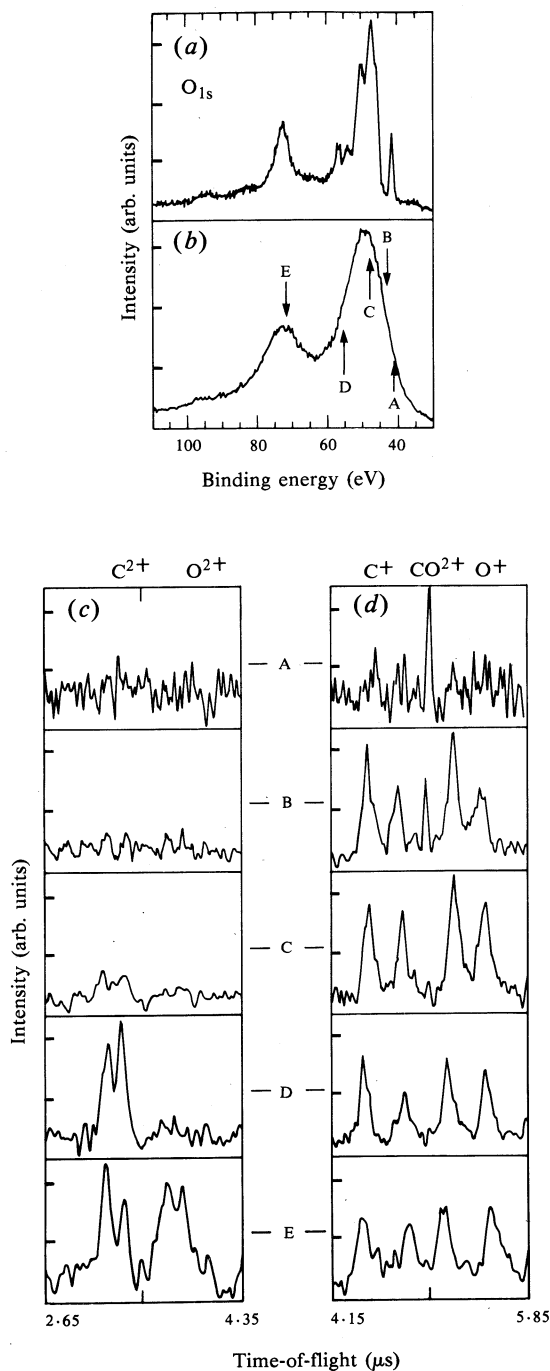


Fig. 7. The TOF ion mass spectra of CO taken in coincidence with oxygen Auger electrons of various kinetic energies as indicated by the arrows A-E in the Auger spectrum (b). A comparison is shown of the Auger spectra taken without (a) and with (b) an ion extractor field applied across the ionisation region. The TOF mass spectra (c) show the region where C^{2+} and O^{2+} are expected to arrive and spectra (d) show the region containing C^+ , CO^{2+} and O^+ .

the $5\sigma^{-1}1\pi^{-1}$ configuration; Correia *et al.* (1985) found that the two lowest Σ states, $X^1\Sigma$ and $B^1\Sigma$, are not very well described by the single particle notation because substantial configuration mixing occurs. Nevertheless, in the following discussion we will largely refer to the states in the single particle notation consistent with earlier theoretical papers (Ågren and Siegbahn 1980; Kelber *et al.* 1981; Liegener 1984; Laramore 1984), keeping the configuration mixing in mind. At position A we are essentially triggering on the $A^1\Pi$ Auger final state and the coincidence spectra show only CO^{2+} . This is consistent with the calculated potential energy curves for the two states contributing to this peak. Both the $X^1\Sigma$ and $A^1\Pi$ states exhibit rather well defined minima in the potential curves (Hurley 1971; Correia *et al.* 1985). These states are actually metastable with respect to decay into C^+ and O^+ . The adiabatic energy for these two fragments is about 5.4 eV lower than the minimum of the $X^1\Sigma$ ground state of CO^{2+} (Hurley 1971). As the subsequent coincidence spectra show, these are the only stable final state configurations of the O Auger decay in CO. Any other double hole configuration in the valence orbitals causes the CO molecule to dissociate.

In coincidence with Auger electrons taken at location B in the oxygen Auger spectrum of CO, we observe now a strong signal of C^+ and O^+ ions in addition to CO^{2+} . The CO^{2+} is most likely a remnant of the previous channel due to the energy smearing of the Auger electrons in the electric field. The C^+ and O^+ ions have to come from the decay of the $1\pi^{-2}$ double hole manifold. Even though we were unable to find any calculated potential energy curves for the resulting Σ and Δ states, it is probably correct to assume that these curves are strongly repulsive because of the bonding character of the 1π electrons. The observed energy of about 7 eV for C^+ and 5 eV for O^+ is consistent with the fact that these states are about 6 eV above the molecular ground state of CO^{2+} . This means that essentially all the excess energy is set free as kinetic energy in the Coulomb explosion. The observed fragment energies for the strongest decay channels are listed in Table 2.

Table 2. Fragment kinetic energies (eV)

Loc. ^A	O Auger				C Auger			
	C^+	O^+	C^{2+}	O^{2+}	C^+	O^+	C^{2+}	O^{2+}
B	7 ± 1	5 ± 1			4.4 ± 1	3 ± 1		
C	8 ± 1	6 ± 1			5 ± 1	4 ± 1		
D	9 ± 2	7 ± 3	9 ± 5				9 ± 3	
E	17 ± 7	15 ± 5	16 ± 8	11 ± 6			13 ± 5	

^A Refers to the location in the coincidence spectra (Figs 7 and 8).

In coincidence with electrons in the largest peak of the oxygen Auger spectrum, location C, the spectra develop as expected. The CO^{2+} signal is completely gone, the dominant species are C^+ and O^+ , and additionally a small amount of C^{2+} is observed. The two hole states are now not only a part of the $1\pi^{-2}$ manifold but contain also the $4\sigma^{-1}1\pi^{-1}$ double hole configurations.

The previously observed trends are confirmed at location D in the Auger spectra where the two hole final states are now largely $4\sigma^{-1}1\pi^{-1}$ and $4\sigma^{-2}$. The C^{2+} signal is very strong and the C^+ and O^+ ions have a larger kinetic energy. We are able to rationalise the development of the ion spectra from the adiabatic energy

scheme, but it nevertheless would be very interesting to have the potential curves available in order to follow the details of this process. Especially the appearance of C^{2+} is not easy to understand in the single particle picture. The initial core hole is created at the oxygen atom and even the Auger final state two hole configurations are predominantly located at the oxygen end of the molecule, the 4σ orbital even more so than the 1π orbital. In a single particle ground state calculation the 4σ orbital has more than 90% of its weight at the oxygen atom. It is hard to imagine that such a hole configuration develops directly into a fragmentation channel as $C^{2+} + O$. On the other hand, one can also take the appearance of C^{2+} in coincidence with these Auger final states as evidence of the substantial configuration mixing in the Auger final states found by Correia *et al.* (1985). These authors pointed out that actually the σ holes are rather delocalised throughout the molecule, which would make the appearance of C^{2+} more likely.

Finally, in coincidence with the 3σ outer valence hole configurations, at location E in the Auger spectrum, we see all four possible fragments, C^{2+} , O^{2+} , and C^+ as well as O^+ with high kinetic energy (see Table 2). We believe these come from the channels $C^{2+} + O$, $O^{2+} + C$, and $C^+ + O^+$ respectively. The fragmentation channels carrying a total charge of three have to undergo an additional Auger transition or electron shake-off event in order to account for the total charge. Probably these events have also a delayed onset compared with the adiabatic thresholds, because of the Coulomb repulsion when the fragments are not separated.

In coincidence with the Auger decay of a C_{1s} core hole in CO we obtained the results shown in Fig. 8. For these studies the fundamental of the undulator was set to 300 eV, rather close to the ionisation threshold. This explains the presence of the deexcitation lines in the Auger spectrum shown in (a). The general similarity between the results obtained at the O edge and at the C edge is not surprising since the final valence hole configurations of the respective Auger decays are largely the same. A few differences, however, should be pointed out.

First, immediately at the top of the C Auger spectrum, there is a strong transition into the $X^1\Sigma$ ground state of CO^{2+} . If we attribute the presence of the C^+ and O^+ signal in the coincidence spectra at A to the energy smearing, then we are able to confirm that this state is also a bound state of CO^{2+} as calculated (Correia *et al.* 1985). Alternately the C^+ and O^+ ions might come from the $C_{1s} \rightarrow 2\pi$ bound state decay, which is in the same energy region and is present as seen by the additional lines in the Auger spectrum.

Second, the C^+ and O^+ signals observed at locations B and C in the coincidence spectra originate from the $B^1\Sigma$ state at a binding energy of about 45 eV. This is in contrast to the situation at the O Auger decay, where the C^+ and O^+ signals come mostly from the decay of the $1\pi^{-2}$ manifold. The $B^1\Sigma$ final state configuration, $4\sigma^{-1}5\sigma^{-1}$, in the single particle notation has, according to Correia *et al.* (1985), only a very shallow minimum. The Franck-Condon region for the transitions from the core hole excited state is located on the repulsive part of this potential curve, such that there is enough energy stored in the system to overcome the very small dissociation barrier. We also note that the fragment energy is smaller than that for the decay of the $1\pi^{-2}$ states seen in the oxygen Auger decay. The measured energies are 4.4 eV (3 eV) for C^+ (O^+). This is consistent with the fact that the potential energy curve of the $B^1\Sigma$ state is about 3 eV lower in energy than the lowest states in the $1\pi^{-2}$ manifold.

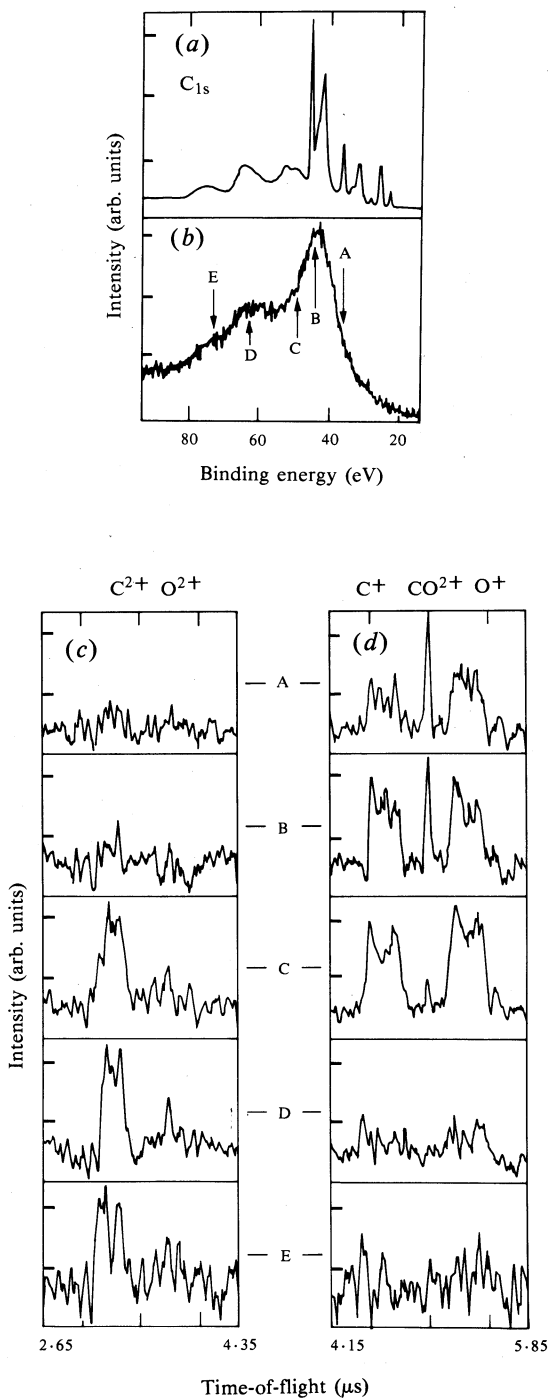


Fig. 8. The TOF ion mass spectra of CO taken in coincidence with carbon Auger electrons (see Fig. 7 for details).

Third, the strong C^{2+} signal at location D occurs at a binding energy of about 55 eV, similar to the situation in the O Auger decay. The $4\sigma^{-2}$ configuration is located at this energy, but it has only a very small amplitude in the C Auger decay. The $4\sigma^{-1}1\pi^{-1}$ configuration on the other hand is almost too close to the adiabatic threshold to account for the large kinetic energy of about 9 eV for the C^{2+} ions. Presently the appearance of this fragment remains a mystery.

The undulator spectrum was rather close to the ionisation threshold for the C_{1s} electrons, which is manifested by the presence of the bound state deexcitation lines in the Auger spectrum. However, neither here nor in our previous studies (Eberhardt *et al.* 1983*b*, 1984, 1985) did we observe any post-collision effects in the fragment spectra. Above the ionisation threshold, the fragment spectra essentially did not change with photon energy, even when we chose the photon energy equivalent to an excitation from the core level into the final state σ shape resonance.

Additionally, secondary decay processes, where a metastable ion travels for a while in the TOF detector before it decays into the final products, are negligible compared with the processes discussed above. This follows from the very low background levels observed in our previous fragmentation studies where we triggered on the unresolved Auger electrons (Eberhardt *et al.* 1983*b*, 1984, 1985).

6. Summary

Even though some questions remain unanswered, we nevertheless obtained a detailed picture of the mechanism leading to the production of ionic fragments following the absorption of a soft X-ray photon. For example, we have identified the $5\sigma^{-2}(X^1\Sigma)$ and the $5\sigma^{-1}1\pi^{-1}(A^1\Pi)$ states as the only stable double hole configurations of CO^{2+} . These studies give new insight into the involvement of individual electrons into the molecular bond, and we are able to correlate the production of certain fragments with the potential energy curves of the doubly charged parent molecules as far as they are available. Consequently, it would be very desirable at this point to have calculations of potential curves available for the higher energy final state configurations as they appear in the Auger spectra.

Acknowledgments

We would like to thank H. Winick, I. Lindau, R. Z. Bachrach and the staff of SSRL for their help and excellent support of the experiment. Special thanks are due to A. Waldhauer, S. Goldberg and B. Pate for helping with the computer programming. This experiment was partially supported by the NSF under Grant No. NSF-DMR-8120331. The SSRL beamline V was funded by NSF Grant No. NSF-DMR-81-08343 and by the Office of Naval Research under N00014-82-C-0722. Research at SSRL is supported by the Department of Energy.

References

- Ågren, H., and Siegbahn, H. (1980). *Chem. Phys. Lett.* **72**, 498.
- Correia, N., Flores-Riveros, A., Ågren, H., Helenelund, K., Asplund, L., and Gelius, U. (1985). *J. Chem. Phys.* **83**, 2036.
- Eberhardt, W., Chen, C. T., Ford, W. K., and Plummer, E. W. (1986). *Aust. J. Phys.* **39**, 853.
- Eberhardt, W., Chen, C. T., Ford, W. K., Plummer, E. W., and Moser, H. R. (1985). In 'DIET II, Springer Series in Surface Science', Vol. 4 (Eds W. Brenig and D. Menzel), p. 50 (Springer: Berlin).

- Eberhardt, W., Sham, T. K., Carr, R., Krummacher, S., Strongin, M., Weng, S. L., and Wesner, D. (1983 *a*). *Phys. Rev. Lett.* **50**, 1038.
- Eberhardt, W., Stöhr, J., Feldhaus, J., Plummer, E. W., and Sette, F. (1983 *b*). *Phys. Rev. Lett.* **51**, 2370.
- Eberhardt, W., Stöhr, J., Troxel, C., Jr, Feldhaus, J., Plummer, E. W., and Sette, F. (1984). *Rev. Sci. Instrum.* **55**, 354.
- Hitchcock, A. P., and Brion, C. E. (1980). *J. Electron Spectrosc. Relat. Phenom.* **18**, 1.
- Hurley, A. C. (1971). *J. Chem. Phys.* **54**, 3656.
- Kay, R. B., Van der Leeuw, Ph.E., and Van der Wiel, M. J. (1977). *J. Phys. B* **10**, 2513.
- Kelber, J. A., Jennison, D. R., and Rye, R. R. (1981). *J. Chem. Phys.* **75**, 652.
- Laramore, G. E. (1984). *Phys. Rev. A* **29**, 23.
- Liegner, C. M. (1984). *Chem. Phys. Lett.* **106**, 201.
- Moddeman, W. E., Carlson, T. A., Krause, M. O., Pullen, B. P., Bull, W. E., and Schweitzer, G. K. (1971). *J. Chem. Phys.* **55**, 2317.
- Moore, C. (1958). Atomic energy levels. National Bureau of Standards, Circular No. 467.
- Shaw, D. A., King, G. C., Cvejanovic, D., and Read, F. H. (1984). *J. Phys. B* **17**, 2091.
- Siegbahn, K., Nordling, C., Johansson, G., Hedman, J., Heden, P. F., Hamrin, K., Gelius, U., Bergmark, T., Werme, L. O., Manne, R., and Baer, Y. (1969). In 'ESCA Applied to Free Molecules' (North-Holland: Amsterdam).

Manuscript received 3 February, accepted 1 August 1986